Proceedings of the 2020 Design of Medical Devices Conference
DMD2020
April 6, 7-9, 2020, Minneapolis, MN, USA

DMD2020-9041

MITIGATING COMPLICATIONS CAUSED BY INTRAVENOUS THERAPY: THE IV PATENCY MONITORING DEVICE

Daniel J. Portillo, Grant Copeland, Bao Huy Vu, Omar Navarro, Gabriela Pineda, Sepehr Seifi, R. Lyle Hood[1]
Department of Mechanical Engineering, The University of Texas at San Antonio
San Antonio, TX, USA

Sukhwinder Kaur
Department of Biomedical Engineering, The University of Texas at San Antonio
San Antonio, TX, USA

Nitin A. Das, Daniel T. DeArmond, John H. Calhoon
Department of Cardiothoracic Surgery, The University of Texas Health Science Center San Antonio
San Antonio, TX, USA

ABSTRACT

Although intravenous therapy (IV) is one of the most frequently utilized approaches for fluid delivery in modern healthcare, it is associated with some form of complication up to 40% of the time. While many complications are minor, occlusion and extravasation can prevent the delivery of a needed fluid-based intervention or cause delivery into the subdermal space, which can lead to distributed tissue damage and necrosis. To address this need, this group developed the IV patency monitoring device (IVP) to generate and analyze a small pulse wave within the IV fluid. The study hypothesis was that changes in the IV's communication with the blood stream could be detected as an alteration in this signal. This study investigated wave characteristics generated by the IVP in a benchtop tissue phantom. Results demonstrated that wave characteristics change detectably between simulated patent communication with a simulated blood stream and states of extravasation or occlusion. Future work will focus on improved detection methods and integrating a real-time alert system, which will better prepare the IVP for clinical translation and impact.

Keywords: Intravenous therapy, IV, patency, occlusion, extravasation, infiltration, IV monitoring

NOMENCLATURE

A	Amperes
A	initial cross-sectional area
$\dot{A}$	rate of change of the cross-sectional area
a	speed of the propagating wave
c	acoustic speed within the tubing (considered to be anchored longitudinally)
D	diameter of the tubing
DI	Deionized
E	Young's modulus of the tubing
e	thickness of the tubing
g	gravitational acceleration
$\dot{H}$	rate of change of the hydraulic head
ΔH	change in hydraulic head
Hz	Hertz
IV	Peripheral intravenous therapy and/or system
IVP	Intravenous patency monitoring device
K	bulk modulus of elasticity
mL	Milliliter
mm	Millimeter
ms	Millisecond
μ	Poisson's ratio of the tubing
ρ	initial density
$\dot{\rho}$	rate of change of the density
$\Delta\rho$	change in density of the fluid
V	Volts
V_x	velocity of the fluid
3D	Three-dimensional
% wt./vol	Percent weight per unit volume

INTRODUCTION

Peripheral intravenous therapy (commonly referred to as an IV) is a method used to deliver liquids into the bloodstream [1]. A catheter is inserted into a peripheral vein and fluid-based therapeutics are delivered by infusion, either via syringe or drip bag. In the United States alone, an estimated 200 million IV devices are placed in hospitals each year for the delivery of fluids and/or medications [2-4]. The most common IV complications

[1] R. Lyle Hood: lyle.hood@utsa.edu, 1 UTSA Circle, San Antonio, TX 78249, (210)-458-7909

are blood clots obstructing the flow (occlusion) and needles slipping out of the vein into the surrounding tissue (extravasation). Both scenarios can result in substantial patient morbidity, such as swelling, phlebitis, discomfort, bloodstream infections, deep vein thrombosis, and even tissue necrosis.

Studies claim that anywhere between 10 – 46% of all IVs induce additional patient morbidity [2, 5-7]. Each of these instances, at a minimum, require the removal and replacement of the IV [8]. In an attempt to mitigate the high occurrence of IV-induced complications, the Center for Disease Control (CDC) has created guidelines for hospitals to adapt labor-intensive algorithms that involve replacing IV lines every 3-4 days [9]. Unfortunately, these practices have not made a sufficient impact in reducing the rate of IV complications [2].

The frequency and severity of these IV-induced complications raises the need for an improved detection and alert system, and some solutions already exist. A few groups have designed devices to reduce the rate of infection, but those devices do not actively monitor the IV [10, 11]. Alternatively, a commercially available technology, the ivWatch® (ivWatch, LLC), has been developed to address some of the more prevalent issues [12]. The device operates by sending and monitoring infrared (IR) light through the subcutaneous tissue in the arm to detect when fluid has entered the tissue surrounding the vein. The most significant problems with this device are variations of patients' anatomy, such as hydration, fat content, vein health, and skin tone. These factors will affect the IR light detection and, at present, have no compensatory mechanism. Furthermore, the device cannot detect occlusion. The ivWatch® also introduces another cable and screen into the care environment, which is already plagued with wires and monitors.

Another commonly available solution is a line pressure monitor, which are placed on the drip bags used during IV treatment to regulate fluid flow. However, these sensors are largely insensitive to extravasation since the pressure change is so minute. In some cases, IV pumps are used to deliver the necessary fluid, but they have been shown to be inaccurate [13].

We propose an innovative IV patency monitoring device (IVP) that will monitor the status of the IV during use and alert caregivers of hazardous scenarios in real-time. The IVP has significant advantages to the solutions currently on the market: 1) it capitalizes on monitoring the fluid within the IV line; 2) it possess calibration features to standardize every instance that it is deployed (obviating patient and fluid variability); 3) it does not alter or interfere with the existing IV system, as it will be mounted externally on the IV line; 4) it does not have a secondary monitoring screen and the alerts will come directly from the device. Due to the enormous reliance on IVs in modern medicine, the IVP also has the potential to save over $10 billion and 20 million staff hours per year at hospitals in the US [14-16].

1.1 Hypothesis

The IVP operates by sending, detecting, and analyzing a small pressure within the IV line. The operating concept relies on the continuous fluid column created by the mixing of blood and the IV fluid being delivered. That fluid column is capable of propagating a small pressure wave, which was validated during preliminary experiments [17]. The IVP integrates a pressure wave generator and a pressure wave detector into a single device attachable to the IV line.

As the IVP monitors the small pulse waves within the IV line, it analyzes the signal created by the vibration sensor to determine when the IV enters a hazardous state. After the IVP identifies that the IV has entered a hazardous state, the IVP will emit an audio and visual alarm for the caretaker. The hypothesis of this work is that the IV fluid will be discriminately altered depending on the patency state of the IV.

MATERIALS AND METHODS

2.1 Prototype Device Design

An electronically controlled linear solenoid (5 V, 1.1 A, 4 mm, Uxcell) was used to create a small pressure wave within the IV line. The firing pin in the linear solenoid was positioned perpendicularly to the IV line and the action of the linear solenoid was controlled by an Arduino Uno. The linear solenoid was programmed to impact the IV line at 6.7 Hz.

A small piezoelectric vibration sensor (MiniSense 100, Measurement Specialties) was initially used to detect the pressure wave being emitted. The vibration sensor was also positioned perpendicularly to the line, and the center axis of the ring on the vibration sensor was parallel to the center axis of the firing pin in the linear solenoid. The analog signal produced by the vibration sensor was captured with a second Arduino Uno at a baud rate of 115,200.

A mount for both the linear solenoid and vibration sensor was designed using Onshape. Then, the model was 3D printed (Tough Resin, Form 2) and the linear solenoid and vibration sensor were fixed upon it. Images of the design and 3D printed sensor mount can be seen in Figure 1.

2.2 Phantom Arm Model

In order to evaluate the prototype of the IVP, a phantom arm model consisting of simulated tissue and vein was fabricated. The phantom mimicked the density and acoustic properties of a human arm, as described by previous groups [18-21]. An acrylic mold was created to hold the hydrogel in a shape similar to a human arm. The phantom tissue (hydrogel) was comprised of deionized (DI) water, 16% wt./vol gelatin (Gelatin from bovine skin, 225 g Bloom, Type B, Sigma-Aldrich), and 2% wt./vol sodium alginate (Alginic acid sodium salt from brown algae, medium viscosity, Sigma-Aldrich). A clear piece of polyvinyl chloride (PVC) tubing was inserted through the acrylic mold before the hydrogel was poured and functioned as a phantom human vein.

The flow through the phantom vein was controlled by a syringe pump (PHD ULTRA Series, MA1 70-3007, Harvard Apparatus) mounted with a 60 mL syringe. The flow through the IV line was controlled by a second syringe pump (Single-syringe infusion pump, Cole-Parmer) mounted with a 10 mL syringe. Both syringes were filled with DI water, and the IV fluid was dyed green to visually validate fluid flow within the vein. The phantom arm model can also be seen in Figure 1.

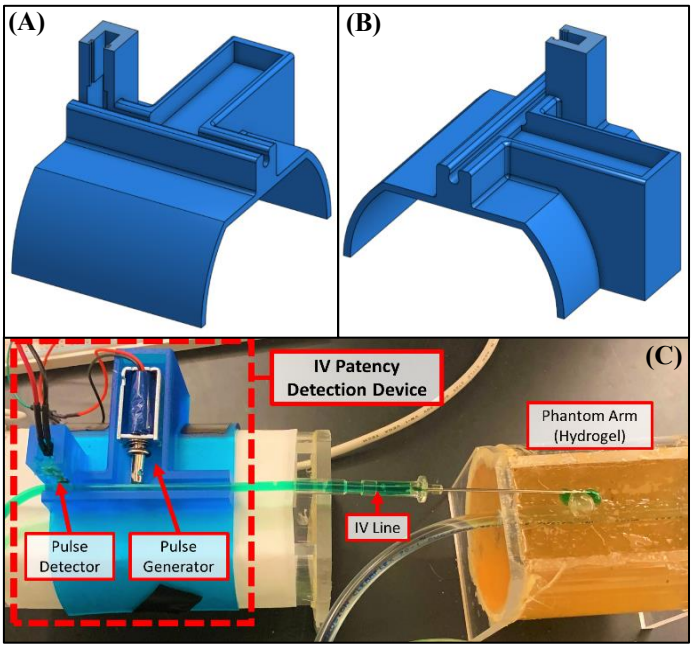

FIGURE 1: (A) ISOMETRIC VIEW OF SENSOR MOUNT MODEL, (B) ALTERNATIVE ISOMETRIC VIEW OF SENSOR MOUNT MODEL, (C) PROTOTYPE OF IVP OUTFITTED WITH PULSE GENERATOR (LINEAR SOLENOID) AND PULSE DETECTOR (PIEZOELECTRIC VIBRATION SENSOR) SITUATED ON 3D PRINTED SENSOR MOUNT; THE PHANTOM ARM MODEL CAN BE SEEN ON THE RIGHT.

2.3 Experimental Procedure

Three scenarios were evaluated: one non-hazardous scenario and two hazardous scenarios. The IV line, outfitted with a 14-gauge needle, was placed inside of the IVP for all three scenarios. The non-hazardous scenario simulated normal flow; the IV needle was inserted into the phantom vein (through the phantom tissue) and both fluids were flowing. The flow rate in the phantom vein was set to 3 mL/min and the flow rate in the IV was set to 2 mL/min.

The first hazardous scenario simulated occlusion; the IV needle was inserted into the phantom vein (through the phantom tissue) and only the IV fluid was flowing. In order to simulate an occlusion, a hemostat was placed on the phantom vein near the insertion point of the IV needle. The flow rate in the IV line was set to 2 mL/min. The second hazardous scenario simulated extravasation; the IV needle was inserted into the phantom tissue (beside the phantom vein) and both fluids were flowing. In this scenario, the flow rate in the phantom vein was set to 3 mL/min and the flow rate in the IV was set to 2 mL/min.

2.4 Data Analysis for Flow Sensor

In order to better characterize the exact changes in flow that the linear solenoid was producing, a flow sensor (SLF3S-1300F, Sensirion) was introduced into the IV line. The flow sensor was positioned between the linear solenoid and the IV needle. The proprietary Sensirion Sensor Viewer Software was used to record data from the flow sensor (at 1000 Hz) and the data was processed using MATLAB. All the three scenarios were tested, and 100 pulses worth of data was captured for each scenario.

2.5 Data Analysis for Vibration Sensor

The data generated by the vibration sensor was collected with Arduino, stored in MS Excel, and processed with MATLAB. Each of the three scenarios was tested 20 times, and each test consisted of 100 small pressure waves (2,000 pressure waves for each scenario). The first step in processing the data from each scenario was to set a floor and ceiling that would remove any unwanted noise. Then, a kernel distribution was created for all remaining values, providing a custom distribution for 2,000 pulses worth of data for each scenario. The purpose for increasing the number of pulses evaluated, relative to the number of pulses evaluated with the flow sensor, was to increase confidence.

RESULTS AND DISCUSSION

3.1 Theoretical Wave Propagation

If the propagating wave, or moving control volume, created by the linear solenoid is considered fixed relative to the tubing, the propagating fluid volume moves only as the inside of the surface of the tubing deforms. A continuity equation for wave propagation, Equation 1, is derived from the law of conservation of mass [22].

$$\frac{\dot{A}}{A} + \frac{\dot{\rho}}{\rho} + V_x = 0 \tag{1}$$

Equation 1 includes terms for the rate of change of the cross-sectional area ($\dot{A}$), the of the initial cross-sectional area (A), the rate of change of the density ($\dot{\rho}$), the initial density (ρ), and the velocity of the fluid (V_x). Equation 1 can also be derived and rewritten to the form shown in Equation 2, which depends on gravitational acceleration (g), the rate of change of the hydraulic head ($\dot{H}$), and the speed of the propagating wave (a).

$$g\dot{H} + a^2 V_x = 0 \tag{2}$$

Equation 2 is derived from Equations 3, 4, and 5, which take into account the bulk modulus of elasticity (K), Young's modulus of the tubing (E), diameter of the tubing (D), thickness of the tubing (e), acoustic speed within the tubing (considered to be anchored longitudinally, c), change in hydraulic head (ΔH), change in density of the fluid ($\Delta\rho$), and Poisson's ratio of the tubing (μ).

$$a^2 = \frac{K/\rho}{1+[(K/E)(D/e)]c} \tag{3}$$

$$K = \frac{\rho g \Delta H}{\Delta\rho/\rho} \tag{4}$$

$$c = \frac{2e}{D}(1+\mu) + \frac{D(1-\mu^2)}{D+e} \tag{5}$$

Utilizing Equations 2 – 5, the calculated speed of wave propagation through the IVP system is expected to be 1.47 m/s. The initial pressure wave propagation is expected to occur at 34.5 ms after the initial increase in flow.

3.2 Results from Flow Sensor

The flow rates for the pulses gathered within each scenario were averaged together (n=100) and compared to the other scenarios, which can be seen in Figure 2. The highest peak values in Figure 2 exhibits the initial propagation wave passing through the flow sensor. The peak values of 45 mL/min generated by the

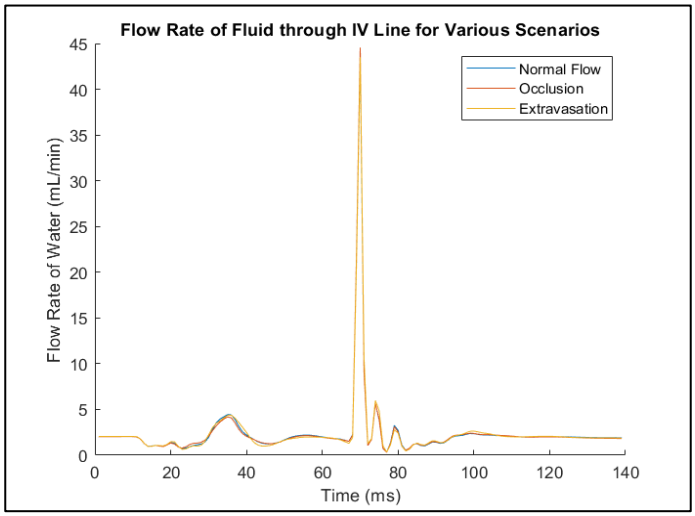

FIGURE 2: FLOW RATE OF DI WATER THROUGH IV LINE FOR NON-HAZARDOUS (NORMAL FLOW) AND HAZARDOUS (OCCLUSION AND EXTRAVASATION) SCENARIOS.

pulse generator are well below the typical 95 – 250 mL/min flow rate within the cephalic vein [23]. The time between the initial peak and the largest pressure wave propagation is 34 ms. Although maximum peak values for each scenario are not confidently distinguishable, there is some distinguishability between scenarios in the time frame of 39 – 49 ms. Figure 3 shows the 39 – 49 ms window from Figure 2 more clearly. The error bars in Figure 3 are the standard deviation values determined from the data set (n=100). The data in Figure 3 was statistically correlated with the two-sample Kolmogorov-Smirnov test. The normal flow and occlusion data had a *p*-value of 0.985 and the normal flow and extravasation data had a *p*-value of 0.147.

Figure 3 shows that the extravasation scenario produced a flow rate that was distinguishable from the normal flow. Figures 2 and 3 also show that the occlusion scenario did not produce a flow rate that was distinguishable from the normal flow. These results partially support the hypothesis, as only one hazardous scenario is distinguishable.

3.3 Results from Vibration Sensor

An example of raw signals recorded from the vibration sensor for each state are shown in Figure 4. Each subfigure shows the data for three small pulse waves. The processed data from the vibration sensor can be seen Figure 5, which shows obvious distinguishability between the non-hazardous and hazardous scenarios, thus confirming the hypothesis. While the flow sensor only showed distinguishability for one hazardous state, the vibration sensor showed distinguishability between both hazardous states. Alternatively, the flow sensor provided higher resolution data than the vibration sensor.

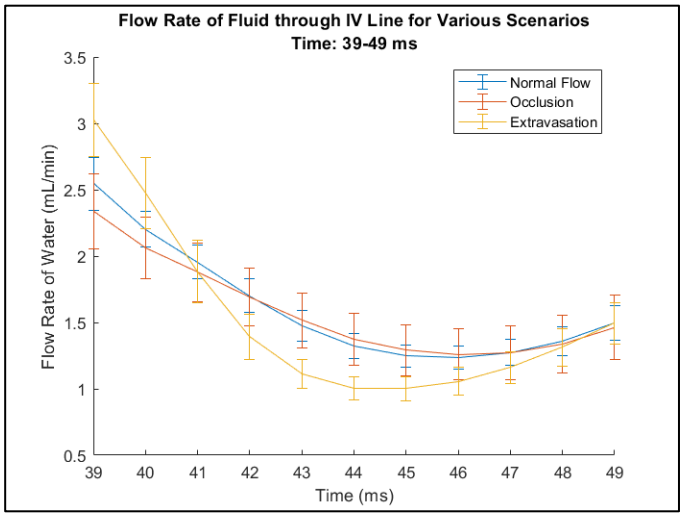

FIGURE 3: FLOW RATE OF DI WATER THROUGH IV LINE FOR NON-HAZARDOUS (NORMAL FLOW) AND HAZARDOUS (OCCLUSION AND EXTRAVASATION) SCENARIOS.

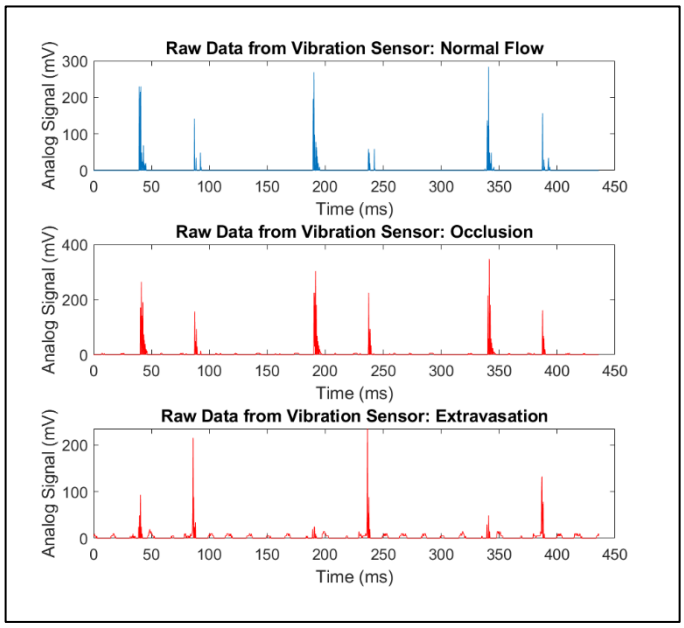

FIGURE 4: ANALOG SIGNAL GENERATED BY THE PIEZOELECTRIC VIBRATION SENSOR FOR NON-HAZARDOUS (BLUE) AND HAZARDOUS (RED) SCENARIOS.

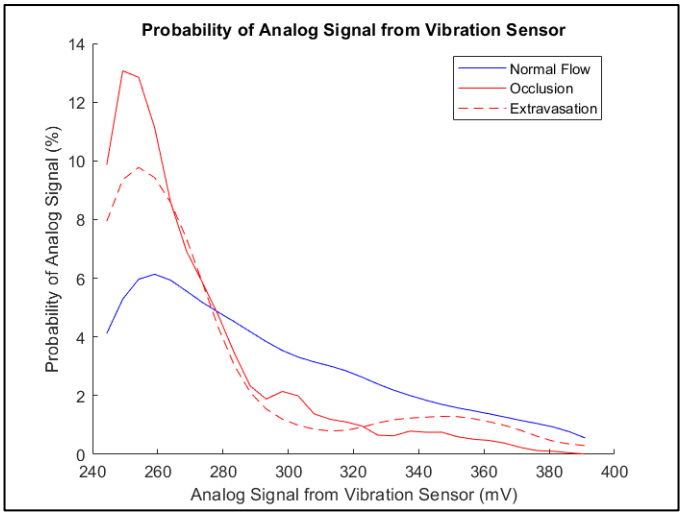

FIGURE 5: PROBABILITY OF ANALOG SIGNAL GENERATED BY THE PIEZOELECTRIC VIBRATION SENSOR FOR NON-HAZARDOUS (BLUE) AND HAZARDOUS (RED) SCENARIOS.

3.3 Discussion and Future Work

Since the variations of flow patterns (related to different scenarios) have been identified, future work related to the IVP will focus on the flow detection methods. The optimal system will incorporate sensors with a high resolution, similar to the flow sensor, and sensors that reliably detect different states. In order to reduce the fabrication cost and maximize the ease of use, the flow detection method will remain external of the IV line, a variation of the device proposed by DeArmond and Calhoon [24]. In order to avoid testing for various other experimental control parameters (i.e. IV placement variability, pulsatile flow in the vein, blood pressure), the IVP will be calibrated to a healthy, patient-specific data set that will be collected immediately after a caretaker has initially placed the IV. Following the calibration, known pulse signals will be administered and data will be gathered at designated intervals, which obviates patient movement or interaction.

Once the flow detection method is solidified, the IVP will be programmed to evaluate the flow data and trigger an alarm system. With these simple systems in place, the IVP will be able to detect when an IV enters a hazardous state and alert a caretaker of the hazard.

CONCLUSION

The prototype of the IVP provided promising benchtop testing results, as it detected changes in signal responses between non-hazardous and hazardous scenarios (occlusion and extravasation). The flow rate within the IV line was characterized for the operation of the IVP, but non-hazardous and hazardous states were not fully distinguishable from the flow rate data (only extravasation was distinguishable). The vibration of the IV line was also evaluated and showed distinguishability between non-hazardous and hazardous states, thus confirming the original hypothesis.

ACKNOWLEDGEMENTS

This work was funded by the Department of Cardiothoracic Surgery at the University of Texas Health Science Center at San Antonio. Additionally, the team would like to thank Vascular Perfusion Solutions, Inc. for providing the flow sensor.

REFERENCES

[1] Waitt, C., Waitt, P., and Pirmohamed, M., 2004, "Intravenous therapy," Postgrad Med. J., **80**(939), pp. 1-6.

[2] Rickard, C. M., Webster, J., Wallis, M. C., Marsh, N., McGrail, M. R., French, V., Foster, L., Gallagher, P., Gowardmen, J. R., Zhang, L., McClymont, A., Whitby, M., 2012, "Routine versus clinically indicated replacement of peripheral intravenous catheters: a randomized controlled equivalence trial," Lancet, **380**(9847), pp. 1066-1074.

[3] Alexandrou, E., Ray-Barruel, G., Carr, P. J., Frost, S., Inwood, S., Higgins, N., Lin, F., Alberto, L., Mermel, L., Rickard, C. M., 2015, "International Prevalence of the Use of Peripheral Intravenous Catheters," Journal of Hospital Medicine, **10**(8), pp. 530-533.

[4] Zingg, W., and Pittet, D., 2009, "Peripheral venous catheters: an under-evaluated problem," International Journal of Antimicrobial Agents, **34**(4), pp. S38-S42.

[5] Helm, R. E., Klausner, J. D., Klemperer, J. D., Flint, L. M., Huang, E., 2015, "Accepted but Unacceptable: Peripheral IV Catheter Failure," Journal of Infusion Nursing, **38**(3), pp. 189-203.

[6] Alexandrou, E., Ray-Barruel, G., Carr, P. J., Frost, S., Inwood, S., Higgins, N., Lin, F., Alberto, L., Mermel, L., Rickard, C. M., 2018, "Use of Short Peripheral Intravenous Catheters: Characteristics, Management, and Outcomes Worldwide," Journal of Hospital Medicine, online, pp. E1-E7.

[7] Webster, J., Clarke, S., Paterson, D. S., Hutton, A., van Dyk, S., Gale, C., Hopkins, T., 2008, "Routine care of peripheral intravenous catheters versus clinically indicated replacement: randomised controlled trial," BMJ, **337**(7662), pp. 157-160.

[8] Doyle, G. R., and McCutcheon, J. A., 2015, Clinical Procedures for Safer Patient Care, BCcampus, Victoria, BC.

[9] O'Grady, N. P., Alexander, M., Burns, L. A., Dellinger, P., Garland, J., Heard, S. O., Lipsett, P. A., Masur, H., Mermel, L. A., Pearson, M. L., Raad, I. I., Randolph, A., Rupp, M. E., Saint, S., Healthcare Infection Control Practices Advisory Committee (HICPAC), 2011, "Guidelines for the Prevention of Intravascular Catheter-Related Infections, 2011," Center for Disease Control and Prevention.

[10] May-Newman, K., Matyska, M. T., Lee, M. N., 2011, "Design and Preliminary Testing of Novel Dual-Chambered Syringe," J. Med. Devices, **5**(2), 021003.

[11] Wax, D. B., and Hill, B., 2017, "Design and Preliminary Testing of Novel Injection Port Contamination Barrier Devices," J. Med. Devices, **11**(3), 034503.

[12] ivWatch Website, accessed November 5, 2019, https://www.ivwatch.com/.

[13] Sucosky, P., Dasi, L. P., Paden, M. L., Fortenberry, J. D., Yoganathan, A. P., 2008, "Assessment of Current and Continuous Hemofiltration Systems and Development of a

Novel Accurate Fluid Management System for Use in Extracorporeal Membrane Oxygenation," J. Med. Devices, **2**(3), 035002.
[14] Tuffaha, H. W., Rickard, C. M., Webster, J., Marsh, N., Gordon, L., et al., 2014, "Cost-effectiveness analysis of clinically indicated versus routine replacement of peripheral intravenous catheters," Applied Health Economic Health Policy, **12**(1), pp. 51-58.
[15] Goff, D. A., Larsen, P., Brinkley, J., Eldridge, D., Newton, D., Hartzog, T., Reigartt, J. R., 2013, "Resource Utilization and Cost of Inserting Peripheral Intravenous Catheters in Hospitalized Children," Hospital Pediatrics, **3**(3), pp. 185-191.
[16] Lineus Medical Website, accessed November 7, 2019, https://lineusmed.com/clinical-info.
[17] DeArmond, D. T., and Calhoon, J. H., 2013, "System of intravenous fluid/medication delivery that employs signature flow amplitudes or frequencies to facilitate the detection of intravenous infiltration," U.S. 20150335820A1.
[18] Mast, T. D., 2000, "Empirical relationships between acoustic parameters in human soft tissues," Acoustical Society of America, **1**(37), pp. 37-42.
[19] Bush, N. L., and Hill, C. R., 1983, "Gelatine-alginate complex gel: A new acoustically tissue-equivalent material," Ultrasound in Med. and Biol., **9**(5), pp. 479-484.
[20] Dabrowska, A. K., Rotaru, G. M., Derler, S., Spano, F., Camenzind, M., Annaheim, S., Stampfli, R., Schmid, M., Rossi, R. M., 2016, "Materials used to simulate physical properties of human skin," Skin Research and Technology, 22, pp. 3-14.
[21] Saari, A., Kasparkova, V., Sedlacek, T., Saha, P., 2013, "On the development and characterisation of crosslinked sodium alginate/gelatin hydrogels," Journal of the Mechanical Behavior of Biomedical Materials, 18, pp. 152-166.
[22] Wylie, E. B., and Streeter, V. L., 1990, Fluid Transients, FEB Press, MI.
[23] Registered Nurses' Association of Ontario, 2005, "Care and Maintenance to Reduce Vascular Access Complications," Appendix C.
[24] DeArmond, D. A., and Calhoon, J. H., 2017 "Signaling Unit Designed to Introduce Vibrational Impulse Patterns into an Intravenous Fluid Column," WO 2017031394.

